Dalton Transactions

PAPER

View Article Online
View Journal | View Issue

Cite this: *Dalton Trans.*, 2015, **44**, 7960

Synthesis and characterization of mixed-valence manganese fluorophosphate and analogues with clathrate-like structures: $Mn^{III}_6F_{12}(PO_3(OH))_8$-$[Na_8(K_x(H_3O)_{4-x}(H_2O)_2)M^{IV}(OH)_6]$ (M^{IV} = Mn, Ti, Ge)†

Wei-Jian Ren,[a] Jing-Quan Wang,[a] Ya-Xi Huang,[a] Zhi-Mei Sun,[b] Yuanming Pan[c] and Jin-Xiao Mi*[a]

Received 12th February 2015,
Accepted 19th March 2015

DOI: 10.1039/c5dt00646e

www.rsc.org/dalton

A novel, mixed- and high-valence manganese (Mn^{3+}/Mn^{4+}) fluorophosphate, $Mn^{III}_6F_{12}(PO_3(OH))_8$-$[Na_8(K_x(H_3O)_{4-x}(H_2O)_2)Mn^{IV}(OH)_6]$ (denoted as **MN**), has been prepared *via* a water-deficient hydrothermal route with phosphoric acid as the sole solvent. This compound features a cubic three-dimensional open-framework structure built from corner-sharing $[Mn^{III}O_4F_2]$ octahedra and $[HPO_4]$ groups, which encapsulates a clathrate-like "guest cluster" of $Na_8(K_x(H_3O)_{4-x}(H_2O)_2)Mn^{IV}(OH)_6$. The guest cluster is architecturally composed of a $[Mn^{IV}(OH)_6]$ octahedron in a cubic cage of Na^+ cations, which in turn is surrounded by an octahedral arrangement of K^+/H_2O ions, resulting in an unprecedented octahedral @ cubic @ octahedral @ cubic arrangement (OCOC). The +4 oxidation state of Mn in the guest cluster has been confirmed by the synthesis of isotypic Ti- and Ge- analogues (denoted as **TI** and **GE**) using TiO_2 and GeO_2 as the replacement for MnO_2 in the starting materials. The compounds **MN**, **TI** and **GE** are not stable in aqueous solution and are peeled off layer-by-layer after the absorption of water. This report provides a new route for the synthesis of mixed- and high-valence manganese phosphates that cannot be produced by conventional hydrothermal methods.

1. Introduction

With the development of novel molecular materials and in-depth studies on the origin and process of life, it is now recognized that many optical,[1] electrical[2] and magnetic properties,[3] as well as superconductivity[4] and electronic transmissions within organisms,[5] are closely related to the mixed-valence phenomenon. Although mixed-valence compounds were produced by chemists a century ago for their unusual color and non-stoichiometric valence, there are only four mixed-valence manganese phosphates among hundreds of inorganic manganese phosphates: $BiMn^{II/III}_6PO_{12}$,[6] bermanite $Mn^{II}(H_2O)_4[Mn^{III}_2(OH)_2(PO_4)_2]$,[7] αββα-$K_3Na_{11}[Mn^{III}_2Mn^{II}_2(H_2O)_2(P_2W_{15}O_{56})_2]\cdot 40H_2O$[8] and $K_{14}Na_{17}[(Mn^{III}_{13}Mn^{II}O_{12}(PO_4)_4(PW_9O_{34})_4]\cdot \sim 56H_2O$.[9] It is also noteworthy that all of these four compounds are the mixtures of Mn^{II} and Mn^{III}, although manganese has diverse valence chemistry: Mn^{II}, Mn^{III}, Mn^{IV}, Mn^{V}, Mn^{VI}, Mn^{VII}, *etc*. High-valence manganese compounds have important applications in oxidation, catalysis and magnetism. However, the instability of high-valence manganese ions in aqueous solution makes the synthesis of these compounds difficult.

To the best of our knowledge, only a few dozen inorganic trivalent manganese phosphates[10] have been reported and there are no tetravalent or higher-valence manganese phosphates, with one exception being polyoxometalate.[11] Thus, in an attempt to enrich the structural chemistry of mixed-valence compounds and obtain high valence manganese compounds, we initiated a comprehensive synthesis program to explore manganese phosphates. The results reported herein demonstrate that we have succeeded in the synthesis of the first-ever, inorganic, mixed- and high-valence manganese phosphate with both Mn^{III} and Mn^{IV}. Mixed Mn^{III} and Mn^{IV} organic com-

[a]*Fujian Provincial Key Laboratory of Advanced Materials, Department of Materials Science and Engineering, College of Materials, Xiamen University, Xiamen 361005, Fujian Province, People's Republic of China. E-mail: jxmi@xmu.edu.cn*
[b]*School of Materials Science and Engineering, Beihang University, Beijing 100191, People's Republic of China*
[c]*Department of Geological Sciences, University of Saskatchewan, 114 Science Place, Saskatoon, SK S7N 5E2, Canada*

†Electronic supplementary information (ESI) available: The figures of experimental and simulated powder X-ray diffraction patterns, EDS/SEM images, TG-DTA, FT-IR and XPS. For ESI and crystallographic data in CIF or other electronic format see DOI: 10.1039/c5dt00646e

pounds are not uncommon.[12] This mixed- and high-valence manganese phosphate $Mn^{III}_6F_{12}(PO_3(OH))_8[Na_8(K_{3.74}(H_3O)_{0.26}(H_2O)_2)Mn^{IV}(OH)_6]$ (denoted as **MN** hereafter) has been synthesized by using a water-deficient hydrothermal method and exhibits a three-dimensional (3D) open-framework structure containing clathrate-like $Na_8(K_{3.74}(H_3O)_{0.26}(H_2O)_2)Mn^{IV}(OH)_6$ guest clusters.

Of particular interest, the structure of the new mixed- and high-valence manganese phosphate resembles that of the clathrate compounds. Clathrates have been known for over two hundred years and are of growing interests for diverse applications from hydrogen storage[13] to superconductivity[14] and semiconductivity,[15] *etc*. These materials possess open framework structures with large cages in the crystal lattice, which can incorporate guest molecules. Previous studies showed that clathrate structures are commonly cubic.[16] The structure of the title compound **MN** is also cubic and is assembled by guest clusters residing in a 3D open framework. The +4 oxidation state of Mn in the guest cluster has been confirmed by the formation of isotypic Ti- and Ge-analogues, $Mn^{III}_6F_{12}(PO_3(OH))_8[Na_8(K_{2.97}(H_3O)_{1.03}(H_2O)_2)Ti(OH)_6]$ and $Mn^{III}_6F_{12}(PO_3(OH))_8[Na_8(K_{2.79}(H_3O)_{1.21}(H_2O)_2)Ge(OH)_6]$ (denoted as **TI** and **GE**), in synthesis experiments using TiO_2 or GeO_2 as starting materials as the replacement for MnO_2. All three isotypic fluorophosphates have been characterized by single X-ray diffraction (XRD) analysis, Fourier-transform infrared spectroscopy (FTIR), X-ray photoelectron spectroscopy (XPS) and magnetic studies.

2. Experimental section

2.1. Synthesis

Reactions of a transition metal fluoride with a phosphate source in a low-water containing, high-fluoride system have been proven to be a powerful route for synthesizing new fluorophosphate compounds.[10,17–19] Here we have synthesized the title compounds *via* a similar water-deficient hydrothermal route with phosphoric acid as the sole solvent. For **MN**, in a typical synthesis procedure, the starting materials of NaF (0.4 g, 9.5 mmol), KPF_6 (0.8 g, 4.3 mmol) and $KMnO_4$ (0.5 g, 3.2 mmol) were dissolved in H_3PO_4 (85%, 1 mL, 14.6 mmol) without adding any water. The resulting mixture with the molar ratio of $NaF : KPF_6 : KMnO_4 : H_3PO_4 = 3 : 1.3 : 1 : 4.6$ was transferred into a 25 mL Teflon-lined stainless-steel autoclave and heated at 240 °C for 3 days under static conditions. The resultant product is composed of crystals in highly viscous gel-like materials. Rosy-red truncated-octahedral crystals in high yields (above 90%, based on Mn, but poor quality) were isolated by filtering after the viscous materials were dissolved in deionized water for a few minutes.

Manganese ions of high oxidation states are well known to be unstable in acidic hydrothermal conditions, *e.g.* $KMnO_4$ spontaneously decomposes to $K_2MnO_4 + MnO_2 + O_2$. Consequently, the high valence Mn^{7+} ions are readily reduced to low valence ions such as Mn^{4+}, Mn^{3+} and Mn^{2+}. In contrast, low-valence manganese ions (*i.e.*, Mn^{2+} or Mn^{3+}) are relatively stable in hydrothermal conditions, and cannot be spontaneously oxidized to high valence ions. It is not possible to synthesize high valence manganese compounds using low valence manganese reactants as starting materials without the addition of high oxidant reagents. In other words, manganese in the starting materials must be tetravalent or higher in valence state in order to synthesize **MN** that contains both trivalent and tetravalent manganese.

As an alternative route for the synthesis of **MN**, we adopted a similar experimental method as above but used MnO_2 (0.278 g, 3.2 mmol) instead of $KMnO_4$ and with the addition of KCl (0.239 g, 3.2 mmol). This method did not produce a single phase but a mixture of high-quality single crystals of **MN** with minor amounts of $KMnF_2(PO_3F)$.[10] The high-quality crystals of **MN** produced *via* this route are suitable for single crystal XRD analysis (see below). Further synthesis investigation shows that Mn_2O_3 or $MnCl_2$ instead of MnO_2 resulted in water-soluble, highly viscous gel-like materials without **MN**. Runs using Mn-metal powder as a starting material produced a new compound $(K_{0.59}(H_3O)_{0.41}Mn^{II}(P(O_{0.5}F_{0.5})_3OH)_2Cl_2$, to be reported elsewhere), supporting the above discussion that the synthesis of the title compound requires high-valence Mn in the starting materials. Hand-picked crystals used for further characterization were first confirmed by a powder X-ray diffraction (PXRD) analysis, which also indicated **MN** to be a new phase and is consistent with the calculated pattern from the single-crystal structure analysis below (Fig. S1†).

Additional synthesis experiments with Ti and Ge have been carried out to confirm that the title compound contains Mn^{IV} as suggested by the single-crystal structure analysis. It is interesting to note that synthesis experiments using the same ingredients and conditions as described above, plus additional TiO_2 or GeO_2 in the stoichiometric proportion, resulted in only the compound **MN** owing to the existence of Mn^{IV}. The Ti and Ge analogues of the title compound (denoted as **TI** and **GE** hereafter) were synthesized by using Mn_2O_3 instead of MnO_2. In a typical synthesis experiment for the compound **TI**, NaF (0.4 g, 9.5 mmol), KPF_6 (0.8 g, 4.3 mmol), KCl (0.239 g, 3.2 mmol), Mn_2O_3 (0.216 g, 1.37 mmol) and TiO_2 (0.036 g, 0.46 mmol) were dissolved in H_3PO_4 (85%, 1 mL, 14.6 mmol). The molar ratio of $NaF/KPF_6/KCl/Mn_2O_3/TiO_2/H_3PO_4$ was about 20.7 : 9.3 : 7.0 : 3.0 : 1.0 : 31.7. Finally, rosy-red truncated-octahedral crystals in high yields (about 90%, based on Ti) were obtained as a pure phase. For the compound **GE**, a similar recipe was used, except that GeO_2 (0.048 g, 0.46 mmol) was added. Rosy-red truncated-octahedral crystals in high yields (about 90%, based on Ge) were also obtained. The PXRD patterns of both **TI** and **GE** are consistent with the calculated ones from the single-crystal X-ray diffraction analyses shown below, and confirm that they are isostructural with **MN** (Fig. S2 and 3†).

2.2. Characterization methodologies

The existence of the Na, K, Mn/Ti/Ge, P, O and F atoms in the title compounds was confirmed by the use of an Energy

Table 1 Crystallographic data and single-crystal X-ray structure refinement results for the compounds **MN**, **TI** and **GE**

	MN	**TI**	**GE**
Formula sum, weight (g mol^{-1})	$F_{12}H_{18.78}K_{3.74}Mn_7Na_8O_{40.26}P_8$, 1853.58	$F_{12}H_{21.10}K_{2.97}Mn_6Na_8O_{41.03}P_8Ti$, 1831.03	$F_{12}GeH_{21.62}K_{2.79}Mn_6Na_8O_{41.21}P_8$, 1852.21
Crystal size (mm^3), color	0.27 × 0.27 × 0.27, rosy-red	0.32 × 0.32 × 0.32, rosy-red	0.30 × 0.30 × 0.30, rosy-red
Crystal system, space-group	Cubic, $Fm\bar{3}$ (no. 202)	Cubic, $Fm\bar{3}$ (no. 202)	Cubic, $Fm\bar{3}$ (no. 202)
Cell parameters (Å)	a = 15.968(2)	a = 16.0001(2)	a = 15.981(7)
Cell volume (Å^3), Z, Calc. density (g cm^{-3})	4071.5, 4, 3.024	4096.05, 4, 2.969	4082, 4, 3.014
Rad., wavelength (Å), temp. (K)	MoKα, 0.71073, 173(2)	MoKα, 0.71073, 173(2)	MoKα, 0.71073, 173(2)
μ (mm^{-1}), F(000)	3.067, 3612	2.858, 3575	3.392, 3609
$2\theta_{max}$ (°), N_{para}	55.86, 43	59.49, 55	57.51, 55
Miller-index	$-20 \le h \le 13$, $-21 \le k \le 20$, $-17 \le l \le 20$	$-21 \le h \le 22$, $-20 \le k \le 15$, $-21 \le l \le 8$	$-21 \le h \le 21$, $-21 \le k \le 9$, $-20 \le l \le 20$
R_{int}, R_1, wR_2	0.025, 0.033, 0.106	0.042, 0.036, 0.112	0.048, 0.042, 0.121
S, N, N ($I > 2\sigma(I)$)	1.184, 462, 394	1.144, 495, 409	1.100, 493, 424
Weight parameters (W_1, W_2)[a]	0.0597, 19.4949	0.0535, 8.1128	0.0648, 45.4995
$\Delta\rho_{max}$, $\Delta\rho_{min}$ (e Å^{-3})	0.780, −0.742	0.955, −0.495	1.317, −0.949

[a] Weight parameters (w = $1/[\sigma^2(F_o^2) + (W_1P)^2 + W_2P]$ where $P = (F_o^2 + 2F_c^2)/3$) were used.

Dispersive X-ray Spectrometer (Oxford Instruments) (Fig. S4–6†). The powder samples checked by PXRD were used for thermal investigations, FTIR and XPS analyses and magnetic measurements. Thermal investigations were performed on a TG-209F1 thermogravimetric/differential thermal analyzer (TG-DTA) in a N_2 atmosphere with a heating rate of 10 K min^{-1}. The FTIR spectra recorded were of powder samples mixed with KBr in pressed pellets on a Nicolet 330 FTIR spectrometer in the range of 400–4000 cm^{-1}. XPS analyses were performed using a Physical Electronics Quantum 2000 scanning ESCA microprobe equipped with a standard focused monochromatic Al Kα (1486.7 eV) X-ray source. Magnetic susceptibility was measured in the temperature range from 2 to 300 K, using a Quantum Design MPMS XL-7 SQUID magnetometer.

2.3. Crystal structure determination

Single crystals of the compounds **MN**, **TI** and **GE** were carefully selected on the basis of clarity and uniformity under a petrographic microscope and were glued onto a thin glass capillary for single-crystal X-ray diffraction analysis. Data collection was performed at 173(2) K, using a Bruker Apex CCD diffractometer or an Oxford Diffraction Xcalibur Sapphire 3 CCD diffractometer, equipped with a graphite-monochromatic MoKα radiation (λ = 0.71073 Å). A total of 6146 observed reflections were collected from 2.21° < θ < 27.93°, yielding 462 unique reflections (R_{int} = 0.025) with 394 $I > 2\sigma(I)$ for the compound **MN**. 2364 observed reflections were collected from 3.60° < θ < 29.75°, yielding 495 unique reflections (R_{int} = 0.042) with 409 $I > 2\sigma(I)$ for the compound **TI**. 6452 observed reflections were collected from 2.21° < θ < 28.75°, yielding 493 unique reflections (R_{int} = 0.048) with 424 $I > 2\sigma(I)$ for the compound **GE**.

The crystal structures of the compounds **MN**, **TI** and **GE** were solved in a cubic space group of $Fm\bar{3}$ by direct methods and refined by the full-matrix least-squares method using the SHELXS-2014 and SHELXL-2014 software packages.[20] The final refinements converged at R_1 [$I > 2\sigma(I)$] = 0.033, 0.036 and 0.042, as well as wR_2 (for all) = 0.106, 0.112 and 0.121 for the compounds **MN**, **TI** and **GE**, respectively. Experimental details for the structure determinations are summarized in Table 1. Detailed information may be found in the ICSD (no. 429030–429032).

3. Results and discussion

3.1. Crystal structure description

The crystal structures of the three compounds, **MN**, **TI** and **GE**, are isotypic and are characterized by $[Mn^{III}O_4F_2]$ octahedra sharing O-corners with $[HPO_4]$ tetrahedra to form a three-dimensional open-framework of $\{Mn^{III}{}_6F_{12}(PO_3(OH))_8\}^{10-}$ with an eight-membered ring channel running along the direction of <100>, in which the $\{Na_8(K_x(H_3O)_{4-x}(H_2O)_2)M^{IV}(OH)_6\}^{10+}$ (M = Mn, Ti, Ge) clusters are encapsulated.

In the crystal structure of **MN**, Mn ions of two different valences (BVS: 3.05 and 4.02 vu.)[21] occur separately at two crystallographically distinct positions: $Mn(1)^{3+}$ and $Mn(2)^{4+}$ at Wyckoff 24d and 4b sites, respectively. Each $Mn(1)^{3+}$ ion is coordinated to four oxygen atoms at 2.066(2) Å and two fluorine atoms at 1.818(2) Å to form a compressed $[Mn(1)^{3+}O_4F_2]$ octahedron, whereas the $Mn(2)^{4+}$ ion is surrounded by six hydroxyl groups (OH) at 1.901(5) Å in a regular octahedron. The compressed $[Mn(1)^{III}O_4F_2]$ octahedron may suggest that the Mn^{3+} ion adopts the high-spin electronic configuration of four unpaired 3d electrons with one electron in one e_g (*i.e.*, $dx^2 - y^2$) orbital. Each $[Mn(1)^{III}O_4F_2]$ octahedron links to four $[HPO_4]$ groups *via* the sharing of equatorial O-corners, and four bidentate Na^+ ions in the axial sides. The $[HPO_4]$ tetrahedron shares

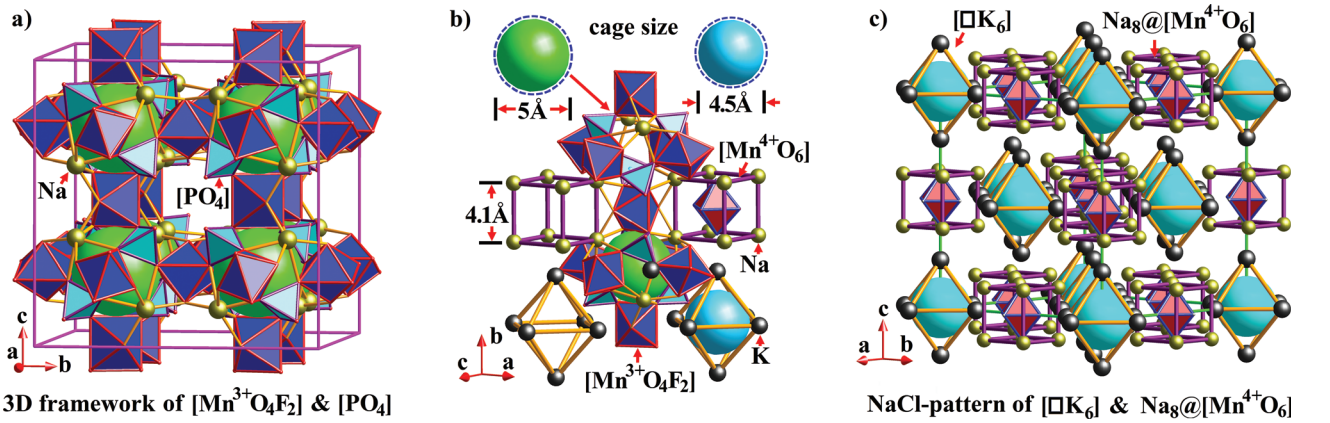

Fig. 1 The crystal structure of **MN**. (a) The framework composed of corner-sharing $[Mn^{III}O_4F_2]$ and $[PO_4]$, with encapsulated cages that are located at the centers of the 8-minicubes of the cubic cell, as F in the fluorite (CaF_2) structure; (b) illustration of the relationship of the framework, cages and guest clusters (the green spheres represent the encapsulated cages in the framework; and the cyan spheres denote the spaces surrounded by six K $(H_3O)/H_2O$ ions); (c) guest clusters and potassium ions in channels arranged in a NaCl-type pattern.

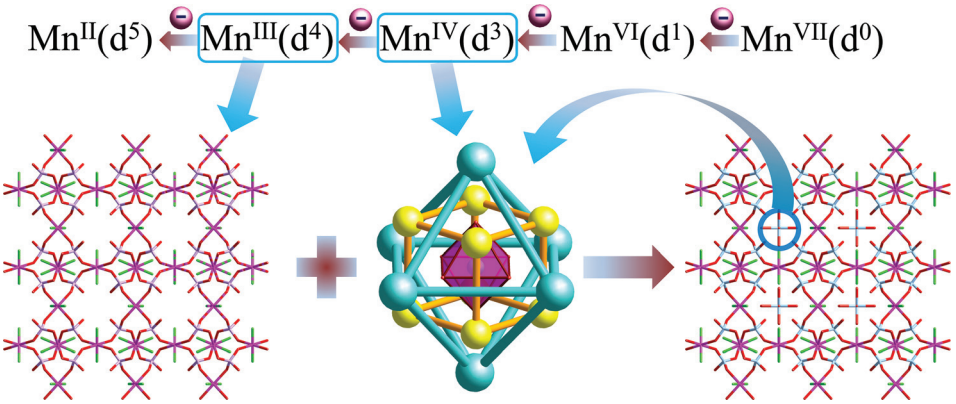

Fig. 2 Illustration of the relationship of the framework and guest clusters. Heptavalent $Mn^{VII}(d^0)$ ions of the starting materials were reduced to low-valence ions: with tetravalent $Mn^{IV}(d^3)$ ions in the guest clusters and trivalent $Mn^{III}(d^4)$ ions forming the framework.

three O-corners, each with a different $[Mn^{III}O_4F_2]$ octahedron, and has a terminal OH group. Each bidentate Na^+ ion also links to three $[Mn^{3+}O_4F_2]$ octahedra. Six neighboring $[Mn(1)^{III}O_4F_2]$ octahedra in octahedral distribution enclose a mini-cube cage, where four involved $[HPO_4]$ groups and four bidentate Na^+ alternately locate at the mini-cube corners in tetrahedral patterns. The mini-cube cage has a diameter of 5.0 Å (Fig. 1). By viewing along the direction of <100>, three-dimensional (3D) interconnected channels contain a narrow 8-membered ring neck consisting of alternating four $[Mn(1)^{III}O_4F_2]$ octahedra and four $[HPO_4]$ groups. The octahedrally distributed K/H_3O ions and water molecules (denoted as $[K_6]$) and the $[Mn^{IV}(OH)_6]@Na_8$ clusters locate within the channels and are arranged in the positions of the NaCl-type structure (Fig. 1). Interestingly, the $[Mn^{IV}(OH)_6]@Na_8$ cluster is octahedrally surrounded by six potassium or water molecules to form a new $[MnO_6]@Na_8@K/H_2O$ cluster in the channels. The $[Mn^{IV}(OH)_6]$ octahedra are not involved in the construction of the 3D open framework structure, and are separated from the framework by Na^+, K^+ and H_2O. As such, the $[Mn^{IV}(OH)_6]$ octahedra and surrounding Na^+, K^+ and H_2O form a clathrate-like "guest cluster" of $Na_8(K_x(H_3O)_{4-x}(H_2O)_2)Mn^{IV}(OH)_6$ (Fig. 2).

3.2. Thermal properties

Thermal analysis of the compound **MN** shows that the first-step weight-loss of 2.32% at the temperature range of 250–450 °C in the TG curve (Fig. S7†) can be ascribed to the removal of 2.39 × H_2O per formula unit (calcd, 2.40%). The powder X-ray diffraction analysis shows that the solid residue of **MN** after annealing at 477 °C for 2 hours mainly consists of Na_2MnPO_4F with a minor amount of $KMnF_3$ and an unidentified phase[22,23] (Fig. S8†).

3.3. Infrared spectroscopy

The FTIR spectra of the compounds **MN** and **TI** show similar absorption bands (see Fig. S9†). The peaks at 3439/3437 cm^{-1}

(medium, broad) can be attributed to the asymmetric O–H stretching, while the peaks at 1620/1640 cm^{-1} (weak, broad) and 3599/3597 cm^{-1} (sharp, weak) are assigned to the H–O–H bending mode. The free PO_4^{3-} ion with the perfect T_d symmetry has four normal modes: $\nu_1(A_1)$, the symmetric stretching mode, $\nu_2(E)$, the OPO symmetric bending mode, and $\nu_3(F_2)$ and $\nu_4(F_2)$, the asymmetric stretching and bending modes, respectively (all Raman allowed, but only ν_3 and ν_4 IR allowed). The bands at 1151/1157 and 1023/1030 cm^{-1} are attributable to the antisymmetric stretching mode (ν_3) of [HPO_4], and those at 585/592 and 517/522 cm^{-1} are ascribed to the antisymmetric bending mode (ν_4). Two inactive IR modes (*i.e.*, ν_1 & ν_2) are not observed, suggesting that the IR forbidden modes are not lifted, and this consistent with the high symmetry of the lattice. The band at 793/826 cm^{-1}, which is beyond the ranges of occurrences for the four normal modes of [HPO_4], may be attributed to the water librations.[24]

3.4. XPS analysis

X-ray photoelectron spectroscopic analysis (Fig. S10†) was performed to identify the oxidation states of manganese and confirm the existence of other elements (*i.e.*, Na, K, F, O, and P) in the compound **MN**. Fig. S10 shows that the XPS spectrum of **MN** exhibits two strong peaks at 642.5 and 653.9 eV in the energy region of Mn $2p_{3/2}$ and Mn $2p_{1/2}$, respectively. The distance between the two main peaks is about 11.4 eV, which may suggest that the manganese mainly has an oxidation state at +3.[25,26] It is noteworthy that the BVS calculations suggest only one Mn^{4+} ion but six Mn^{3+} ions per formula unit in the compound **MN**, and thus the signal of the former in the XPS spectrum is probably overshadowed by the much more abundant Mn^{3+}.

3.5. Magnetic properties

Compounds **MN** and **TI** show linear Curie–Weiss behavior in the χ^{-1} *vs.* T data in the entire 2–300 K temperature range, yielding C_1 = 20.33 emu K mol^{-1}, θ_{C_1} = −2.2 K and C_2 = 18.35 emu K mol^{-1}, θ_{C_2} = −2.7 K, respectively (Fig. 3). The observed effective moment $\mu_{eff1} = 12.75\mu_B$ for the compound **MN** is in excellent agreement with the predicted value of $12.61\mu_B$, assuming a spin-only J value for one Mn^{4+} and six high-spin Mn^{3+} ions. Considering the d^0 state of Ti^{4+}, the observed effective moment $\mu_{eff2} = 12.11\mu_B$ for the compound **TI** is also in good agreement with the predicted value of $12.00\mu_B$, assuming a spin-only J value for six high-spin Mn^{3+} ions. Weak antiferromagnetic (AF) Mn–Mn interactions are expected to predominate in both compounds, which explains the small negative Weiss temperatures, as observed. The gradual increase in the χT product *versus* temperature also conforms to the AF couplings.

3.6. Structural flexibilities and stabilities

The ideal phosphate ion, PO_4^{3-}, has four O^{2-} ions arranged at the corners of a regular tetrahedron. In the compound **MN**, however, each phosphorus atom is split into two positions, and correspondingly, one of the oxygen atoms is also distributed in two sites. This disordered distribution of the [HPO_4] tetrahedron is supposedly caused by self-adjusting of the fundamental building units for fitting the whole structure. As described above, the "guest cluster" of [$Mn^{IV}(OH)_6$] in the channel can be substituted by [$Ge(OH)_6$] or [$Ti(OH)_6$] to form the isotypic compounds of **TI** and **GE**. In both compounds **TI** and **GE**, there is a small residue peak observed around the P-positions, suggesting that a slight disorder of the [HPO_4] tetrahedra also occurs in **TI** and **GE**. However, the occupancies of the disordered P atoms are less than 5% in those compounds; they can be considered to be in an almost fully ordered arrangement. In contrast to **MN**, the P atoms in **TI** and **GE** are

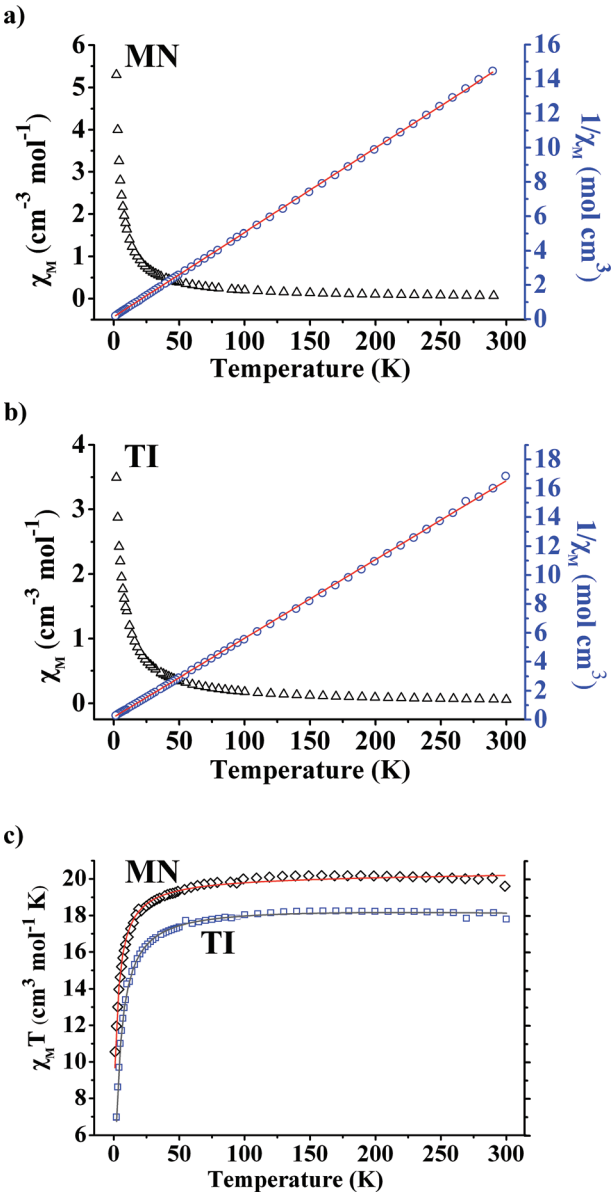

Fig. 3 Magnetic properties of the compounds **MN** and **TI**. Magnetic susceptibility (χ_M) and reciprocal susceptibility (χ^{-1}) *vs.* temperature at 1000 Oe for **MN** (a) and **TI** (b), respectively; their $\chi_M T$ product *vs.* temperature (c).

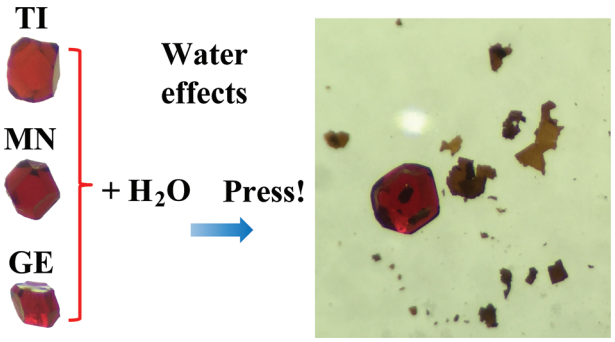

Fig. 4 Illustration of the decomposition of the title compounds in water. All crystals of **MN**, **TI** and **GE** peeled off layer-by-layer after soaking in aqueous solution for 1 hour.

nearly fully ordered in the framework, but the "guest clusters" in the channel are disordered. Every oxygen atom (24e) in the $[Ti^{IV}(OH)_6]$ or $[Ge^{IV}(OH)_6]$ octahedron is split into three positions: at Wyckoff 24e, 48h and 48h sites, respectively. So the crystal structures of the title compounds have high structural flexibilities, which are tuned by order and disorder alteration.

It is interesting to note that the crystals of **MN**, **TI** and **GE** are highly unstable in aqueous solution. When the crystals were soaked in water for one hour, they were peeled off layer-by-layer along {100} and {111} after being pressed slightly (Fig. 4). This pattern of dissolution is observed in all three title compounds, **MN**, **TI** and **GE**, and suggests a preferential removal of the channel constituent oriented along {100}. This suggestion is further supported by the presence of minor crystalline Na(OH) and K_2SiF_6 in the dissolved glassware, although the majority of the solid dissolution products from the title compounds are amorphous (Fig. S11†). Such instability of the title compounds in aqueous solution is not unexpected and is consistent with the fact that high-valence manganese phosphates cannot be synthesized under normal hydrothermal conditions. The successful syntheses of the title compounds in the present study are attributable to our usage of phosphoric acid as the sole solvent under water-deficient hydrothermal conditions. Our previous works have shown that the water content is a crucial factor in the synthesis of other chloride,[27] phosphate[28] and borate[29] compounds.

4. Conclusions

In this paper, we have demonstrated three isotypic new compounds: $Mn^{III}{}_6F_{12}(PO_3(OH))_8[Na_8(K_x(H_3O)_{4-x}(H_2O)_2)M^{IV}(OH)_6]$ (M^{IV} = Mn, Ti, Ge). The first-ever, mixed- and high-valence manganese fluorophosphate with both Mn^{3+} and Mn^{4+} has been synthesized by a water-deficient hydrothermal method with phosphoric acid as the sole solvent. This compound features a clathrate-like structure with a cubic three-dimensional open-framework structure encapsulating the unprecedented $Na_8(K_{3.74}(H_3O)_{0.26}(H_2O)_2)Mn^{IV}(OH)_6$ guest clusters in the channels. Successful syntheses of the isotypic compounds **TI** and **GE** confirm the presence of Mn^{4+} in the guest clusters. This report provides a new hydrothermal route for the synthesis of mixed- and high-valence manganese compounds.

Acknowledgements

This work is supported by the National Science Foundation for Distinguished Young Scientists of China (Grant no. 51225205), the National Natural Science Foundation of China (no. 21233004, 61274005 and 21201144), the Fundamental Research Funds for the Central Universities (no. 2013121020) and financial support from the Natural Science and Engineering Research Council of Canada.

References

1 B. S. Brunschwig, C. Creutz and N. Sutin, *Chem. Soc. Rev.*, 2002, **31**, 168–184.
2 E. G. Walton, P. J. Corvan, D. B. Brown and P. Day, *Inorg. Chem.*, 1976, **15**, 1737–1739.
3 M. Viret, L. Ranno and J. M. D. Coey, *Phys. Rev. B: Condens. Matter*, 1997, **55**, 8067–8070.
4 S. P. Pai, J. Jasudasan, P. R. Apte, R. Pinto, J. Kurian, P. K. Sajith, J. James and J. Koshy, *Europhys. Lett.*, 1997, **39**, 669–673.
5 M. Di Vaira, F. Mani and P. Stoppioni, *J. Chem. Soc., Dalton Trans.*, 1997, 1375–1379.
6 O. Cousin, O. Mentre, M. Huve and F. Abraham, *J. Solid State Chem.*, 2001, **157**, 123–133.
7 A. R. Kampf and P. B. Moore, *Am. Mineral.*, 1976, **61**, 1241–1248.
8 S. Yao, J. H. Yan, Y. C. Yu and E. B. Wang, *J. Coord. Chem.*, 2012, **65**, 1451–1458.
9 Q. Wu, Y. G. Li, Y. H. Wang, E. B. Wang, Z. M. Zhang and R. Clerac, *Inorg. Chem.*, 2009, **48**, 1606–1612.
10 J. A. Armstrong, E. R. Williams and M. T. Weller, *Dalton Trans.*, 2013, **42**, 2302–2308.
11 X. K. Fang and P. Koegerler, *Angew. Chem., Int. Ed.*, 2008, **47**, 8123–8126.
12 C. Lampropoulos, A. E. Thuijs, K. J. Mitchell, K. A. Abboud and G. Christou, *Inorg. Chem.*, 2014, **53**, 6805–6816.
13 H. Lee, J. W. Lee, D. Y. Kim, J. Park, Y. T. Seo, H. Zeng, I. L. Moudrakovski, C. I. Ratcliffe and J. A. Ripmeester, *Nature*, 2005, **434**, 743–746.
14 H. Kawaji, H. Horie, S. Yamanaka and M. Ishikawa, *Phys. Rev. Lett.*, 1995, **74**, 1427–1429.
15 G. S. Nolas, T. J. R. Weakley and J. L. Cohn, *Chem. Mater.*, 1999, **11**, 2470–2473.
16 J. A. Ripmeester, J. S. Tse, C. I. Ratcliffe and B. M. Powell, *Nature*, 1987, **325**, 135–136.
17 J. A. Armstrong, E. R. Williams and M. T. Weller, *J. Am. Chem. Soc.*, 2011, **133**, 8252–8263.
18 A. C. Keates, J. A. Armstrong and M. T. Weller, *Dalton Trans.*, 2013, **42**, 10715–10724.

19 J. A. Armstrong, E. R. Williams and M. T. Weller, *Dalton Trans.*, 2012, **41**, 14180–14187.
20 G. M. Sheldrick, *Acta Crystallogr., Sect. A: Fundam. Crystallogr.*, 2008, **64**, 112–122.
21 N. E. Brese and M. O'Keeffe, *Acta Crystallogr., Sect. B: Struct. Sci.*, 1991, **47**, 192–197.
22 O. V. Yakubovich, O. V. Karimova and O. K. Melnikov, *Acta Crystallogr., Sect. C: Cryst. Struct. Commun.*, 1997, **53**, 395–397.
23 K. Knox, *Acta Crystallogr.*, 1961, **14**, 583–585.
24 V. G. Koleva, *Spectrochim. Acta, Part A*, 2007, **66**, 413–418.
25 Y. F. Han, F. X. Chen, Z. Y. Zhong, K. Ramesh, L. W. Chen and E. Widjaja, *J. Phys. Chem. B*, 2006, **110**, 24450–24456.
26 F. Moro, V. Corradini, M. Evangelisti, V. De Renzi, R. Biagi, U. del Pennino, C. J. Milios, L. F. Jones and E. K. Brechin, *J. Phys. Chem. B*, 2008, **112**, 9729–9735.
27 T. T. Zhu, W. Sun, Y. X. Huang, Z. M. Sun, Y. M. Pan, L. Balents and J. X. Mi, *J. Mater. Chem. C*, 2014, **2**, 8170–8178.
28 L. Z. Sun, W. Sun, W. J. Ren, J. Y. Zhang, Y. X. Huang, Z. M. Sun, Y. M. Pan and J. X. Mi, *J. Solid State Chem.*, 2014, **212**, 48–57.
29 B. C. Zhao, W. Sun, W. J. Ren, Y. X. Huang, Z. C. Li, Y. M. Pan and J. X. Mi, *J. Solid State Chem.*, 2013, **206**, 91–98.